

## **Impact properties of carbon fiber reinforced linear and short-chain branched polyethylenes**

**J.T. Yeh\*, Bih-June Chen, and Hsing-Min Lee**

Graduate School of Textile and Polymer Engineering, National Taiwan Institute of Technology, Republic of China

### **Summary**

An investigation of the influence of short-chain branched length on impact behavior of linear high density polyethylene (HDPE), short-chain branched polyethylenes (SBPEs) and their fiber reinforced samples is reported. The result shows that the total impact energies ( $E_t$ ) increased with increasing branch length at any given temperature used in this study. Similar trend was found for their fiber reinforced samples. For a given polyethylene resin,  $E_t$  increased with fiber content up to 5%, and then decreased consistently with further increase of fiber content. The amount of  $E_t$  improved due to the presence of 5% carbon fibers increased significantly with the branch length at temperatures higher than 25°C. In addition, the fracture surface morphology indicated that the adhesion between carbon fibers and PE resins increased with the branch length. However, the adhesion and the amount of  $E_t$  improved due to the presence of 5% carbon fibers reduced significantly with decreasing temperature. Finally, it was found that  $E_t$  decreased slightly with rising temperature until the temperature reached around 40°C, and then increased sharply with increasing temperature. It is suggested that this "transition" behavior is related to the molecular motion accounting for the  $\alpha$  transition of PE resins.

### **Introduction**

The most common fiber reinforced thermoplastics are made of glass fibers with polyolefins or polyamides as matrices (1). In addition to glass fibers, other fibers such as carbon fibers are also used (2). The consumption of polyolefins used in reinforced thermoplastics increased about 18 times from 1970 to 1980, and that of polyamides increased about 5 times (3). Many traditional polyolefins, such as, high density polyethylene (HDPE), low density polyethylene (LDPE) and polypropylene (PP) have

\* Corresponding author



determined by using the method suggested by ASTM D2584-68. The coated fibers were cut into 6mm in length, and then injection-molded as a circular plaque with dimensions of 51mm in diameter and 3.1mm in thickness at 100°C for various amounts of time. The dimensions of these circular plaques were the standard dimensions of a falling weight impact specimen as suggested by ASTM D3029. After the required crystallization time, the samples were air cooled to 35°C. The average length of the carbon fiber was found to decrease to about 3mm in these circular plaques, which was possibly due to the fact that the carbon fiber was broken in the screw extruder during injection-molding process.

#### Molecular and microstructural characterization

The branch type and frequency of each plain resin were determined by using Burker MSL-200 <sup>13</sup>C-NMR spectrometer operating at 50 MHz. The branch frequencies of each plain resin were determined by using the method proposed by Pooter et. al. (9). The molecular weight and its distribution associated with each plain resin were determined by a Viscotek gel permeation chromatography (GPC) model Sigma 1.0. A DMA unit model Eplexor 150N (GABO Qualimeter Testanlagen GMBH) was used to study the mechanical relaxation behavior of all samples. All DMA experiments were operated at a frequency of 3.5Hz, a heating rate of 3°C/min and the temperature ranged from -150°C to 100°C. The thermal behavior of each plain resin was performed on a Dupont differential scanning calorimeter (DSC) model 2000. The tie molecule density of each plain resin was evaluated from the brittle fracture stress measurements as proposed by Brown and Ward (10).

#### Instrumented falling weight impact test and fracture surface morphology

All falling weight impact experiments were performed on a Hung- sun impact tester model 208. The temperatures used in this study were -50, -20, 0, 25, 50 and 75°C. The impact energy was calculated by determining the area under the force versus displacement graph. The circular plaques prepared in "Materials and preparation" section were used as test specimens and were supported by an annular anvil with an internal diameter of 37.5mm. The fracture surfaces of the impacted specimens were examined using a JOEL JSM-5200 scanning electron microscope (SEM).

## **Results**

### Molecular and microstructural characterization of PE resins

Table 1 summarized the chemical shift assignments of the <sup>13</sup>C-NMR of samples A<sub>0</sub>, B<sub>0</sub> and C<sub>0</sub>. By focusing on samples B<sub>0</sub> and C<sub>0</sub> first, in addition to the assignment corresponding to the major backbone methylene carbon resonance at 30.0 ppm, assignments corresponding to different types of branches were found. No significant difference in the chemical shift assignments was found for samples B<sub>0</sub> and C<sub>0</sub> with those of samples with ethyl and hexyl branches, respectively (see Table 1). These results suggested that samples B<sub>0</sub> and C<sub>0</sub> are associated with ethyl and hexyl types of short-chain branches, respectively. The branch frequency of samples B<sub>0</sub> and C<sub>0</sub> estimated from Pooter's method (9) is approximately 18 branches/1000 carbon atoms. In contrast to sample B<sub>0</sub> and C<sub>0</sub>, no chemical shift assignments associated with any type of branch was found in <sup>13</sup>C-NMR spectrum of sample A<sub>0</sub>. In fact, the chemical shift assignments of sample A<sub>0</sub> are the same as those of the linear HDPE polymer (see Table 1).

Table 1.  $^{13}\text{C}$  NMR chemical shift assignments of A<sub>0</sub>, B<sub>0</sub> and C<sub>0</sub>.

Sample	type of branch	$\delta(\text{ppm})^{\text{a, b}}$												
		br	1s	2s	3s	$\alpha$	$\beta$	$\gamma$	1	2	3	4	5	6
A <sub>0</sub>	linear HDPE		14.1	22.9	32.2									
			(14.1)	(22.9)	(32.2)									
B <sub>0</sub>	ethyl	39.8				34.1	27.4	30.5	11.2	26.8				
		(39.7)				(34.1)	(27.1)	(30.5)	(11.2)	(26.7)				
C <sub>0</sub>	hexyl	38.3				34.6	27.3	30.5	14.1	22.9	32.2	30.0	27.3	34.6
		(38.2)				(34.4)	(27.3)	(30.5)	(14.1)	(22.9)	(32.2)	(30.0)	(27.3)	(34.6)

a: Referred to the isolated methylene resonance at 30.3 ppm.

b: Nomenclature adopted for the assignment of individual carbons.

( ): The values in parenthesis are the chemical shift assignments determined by Pooter and coauthors (9) for linear HDPE and samples associated with typical ethyl and hexyl branches, respectively.

The weight average molecular weights (MW) of samples A<sub>0</sub>, B<sub>0</sub> and C<sub>0</sub> obtained from GPC measurements were 90000, 92000 and 97000, respectively, and the molecular weight distribution (MWD) associated with these samples was about the same and at a value of 3.4. The weight average molecular weight increases slightly for samples with longer branch length, however, the difference is not significant. In fact, this increase may reflect the increase in lengths of short-chain branches rather than that of the main chain of SBPEs. The degree of crystallinity ( $W_c$ ) and tie molecule density ( $f_T$ ) derived from brittle fracture stress measurements (10) of sample A<sub>0</sub> are associated with a value of 76% and 3.1%, respectively. In contrast,  $W_c$  and  $f_T$  of the branched polyethylene samples (i.e., B<sub>0</sub> and C<sub>0</sub>) are approximately the same and are associated with a value of 42% and 6.2%, respectively, which are significant different from those of sample A<sub>0</sub>. This is probably due to the presence of the short-chain branches, which prohibits the incorporation of polymer chains into the crystals and prohibits disentanglements in the amorphous region during crystallization, and hence, results in a lower  $W_c$  and higher  $f_T$ .

#### Dynamic mechanical analysis

The temperature dependence of the storage modulus  $E'$ ,  $\tan\delta$  and the loss modulus  $E''$  for samples A<sub>0</sub>, B<sub>0</sub> and C<sub>0</sub> is shown in Fig. 2. Three distinct transitions were observed as  $E''$  peaks at temperatures near  $-120^\circ\text{C}$  ( $\gamma$  transition),  $-20^\circ\text{C}$  ( $\beta$  transition) and  $45^\circ\text{C}$  ( $\alpha$  transition) in all of the curves of samples B<sub>0</sub> and C<sub>0</sub>. However, only  $\alpha$  and  $\gamma$  transitions were found on the curves of sample A<sub>0</sub>. Similar relaxation behavior was found for the fiber reinforced sample A series (i.e., A<sub>05</sub>, A<sub>15</sub> and A<sub>25</sub>), B series (i.e., B<sub>05</sub>, B<sub>15</sub> and B<sub>25</sub>) and C series (i.e., C<sub>05</sub>, C<sub>15</sub> and C<sub>25</sub>). The transition temperatures remained approximately the same with varying fiber contents.

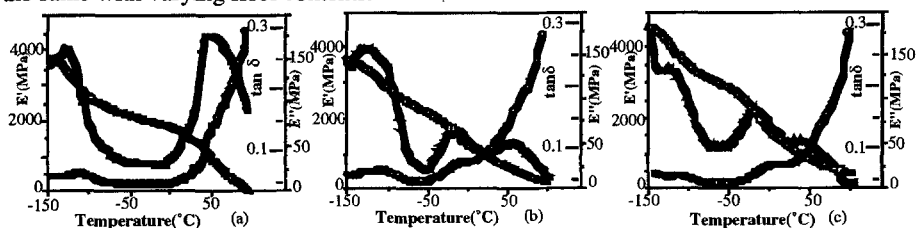


Fig. 2. Dynamic mechanical spectra of samples (a) A<sub>0</sub>, (b) B<sub>0</sub> and (c) C<sub>0</sub>

( $E'$ ( $\square$ -),  $E''$ ( $\diamond$ -),  $\tan\delta$ ( $\circ$ -)).

### Impact experiments

The total impact energies ( $E_t$ ) of all samples tested at different temperatures are shown in Fig. 3. It is interesting to note that  $E_t$  of the plain samples increased from  $A_0$  to  $B_0$  and  $C_0$  at any given temperature. Similar to those of plain PE sample series (i.e.,  $A_0$ ,  $B_0$  and  $C_0$ ),  $E_t$  of the fiber reinforced samples also increased from  $A_x$  to  $B_x$  and  $C_x$  sample series at any fixed fiber content and temperature used in this study.

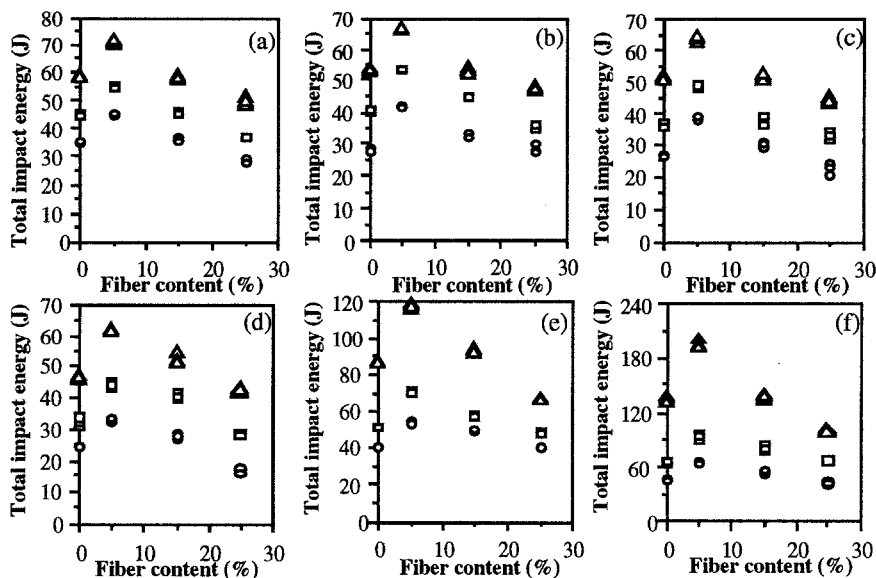


Fig. 3. The total impact energy against fiber content of samples  $A_x$ (○),  $B_x$ (□) and  $C_x$ (△) series at (a)-50, (b)-20, (c)0, (d)25, (e)50 and (f)75°C.

On the other hand, the total impact energies of  $A_x$ ,  $B_x$  and  $C_x$  sample series increased with the content of carbon fiber up to 5%, and then decreased consistently with further increase of fiber content at any temperature used in this study. This is probably because that carbon fibers were not well dispersed in PE matrix at high fiber contents, and resulted in a poor adhesion between the PE resins and carbon fibers. In addition, it is interesting to note that the amount of  $E_t$  improved due to the presence of 5% carbon fibers increased significantly with increasing branch length (i.e., from  $A_x$  to  $B_x$  and  $C_x$  series) at temperatures equal or higher than 25°C. Fig. 4 shows the amounts of  $E_t$  improved at each temperature due to the presence of 5% carbon fiber content.

Fig. 5 shows  $E_t$  as a function of temperature for all samples. In all cases, the total impact energies decreased slightly with rising temperature until the temperature reached around 40°C, and then increased sharply with further increasing temperature. Similar temperature dependence of  $E_t$  of some other SBPE polymers was also observed by Liu and Baker (11). It is not completely understood why  $E_t$  decreased slightly with increasing temperature, and what are the underlying mechanisms accounting for the sharply rise of  $E_t$  at this "transition" temperature (see Fig. 5). However, it is speculated that the "transition" behavior is related to the molecular motion accounting for the  $\alpha$  transition of PE resins,

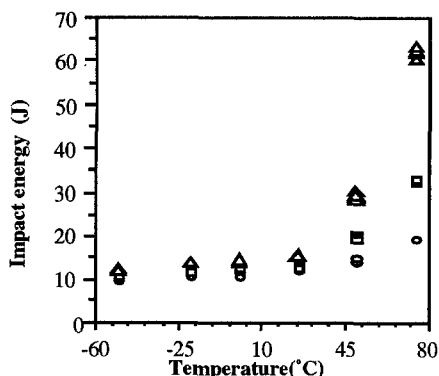


Fig. 4. The improvement of total impact energy of samples A05( $\circ$ ), B05( $\square$ ) and C05( $\Delta$ ) due to the presence of 5% carbon fiber at various temperatures.

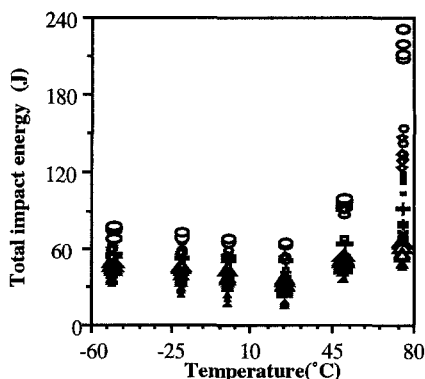


Fig. 5. The total impact energies of samples A0( $\Delta$ ), A05( $\Delta$ ), A15( $\Delta$ ), A25( $\Delta$ ); B0( $\times$ ), B05(+), B15(+), B25(+); C0( $\circ$ ), C05( $\circ$ ), C15( $\diamond$ ), C25( $\square$ ) against temperature.

since the "transition" temperature is very close to the  $\alpha$  transition temperature of the PE resins determined in this study.

## Discussion

### Effect of molecular and crystalline microstructure on $E_t$ of plain PEs and its fiber reinforced samples

The above results show that the total impact energies ( $E_t$ ) of the plain resins or the fiber reinforced samples increased from  $A_x$  to  $B_x$  and  $C_x$  sample series at any given temperature used in this study. The phenomenon is explained due to the difference in the molecular and crystalline microstructure of PE resins and the different degree of adhesion between carbon fibers and PE resins. As mentioned previously, samples  $A_0$ ,  $B_0$  and  $C_0$  are associated with about the same MW and MWD, and samples  $B_0$  and  $C_0$  have the same tie molecule density and branch frequency, but the branch length of sample  $C_0$  is longer than that of sample  $B_0$ . The linear sample,  $A_0$ , is associated with a lower tie molecule density than that of the short-chain branched samples (i.e.  $B_0$  and  $C_0$ ). These results suggested that the improvement in  $E_t$  from sample  $B_0$  to  $C_0$  is possibly due to the increasing sliding resistance of polymer chains through the crystal and through the entanglements in the amorphous region as the length of short-chain branch increases (5, 6). The improvement in  $E_t$  from sample  $A_0$  to  $B_0$  and/or  $C_0$  is possibly due to the increase in tie molecule density and the higher sliding resistance of pulling the short-chain branched molecules through the crystal and entanglements regions than that of the linear molecules.

### Effect of adhesion between carbon fibers and PE resins on $E_t$ of fiber reinforced samples

Further investigation on the fracture surfaces of the impacted specimens showed that samples  $A_x$  series were associated with more voids due to fiber pull-out than those of  $B_x$  and  $C_x$  series and the amount of PE residue adhered to carbon fibers increased with increasing branch length of the plain PE resins (see Figs. 6-8). These results suggested that the titanate coupling agent (CA) improves the adhesion between the SBPE resins and carbon fibers more than that of HDPE and the adhesion is better for SBPE resins associated with longer branch length. It is not completely clear at this point why SBPE

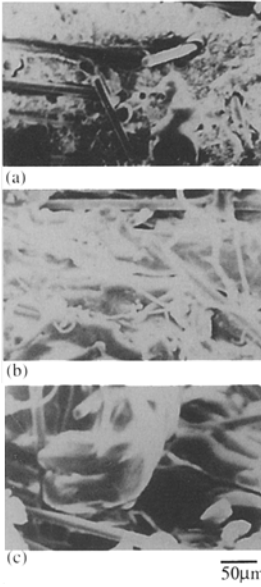


Fig. 6. Fracture surface of samples (a) A<sub>05</sub>, (b) B<sub>05</sub>, (c) C<sub>05</sub> at 75°C.

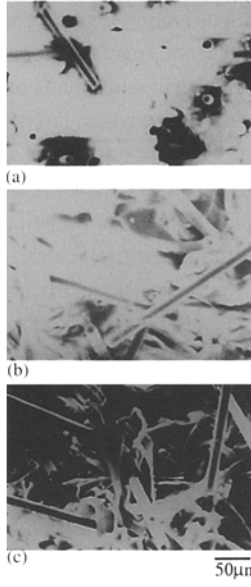


Fig. 7. Fracture surface of samples (a) A<sub>05</sub>, (b) B<sub>05</sub>, (c) C<sub>05</sub> at 50°C.

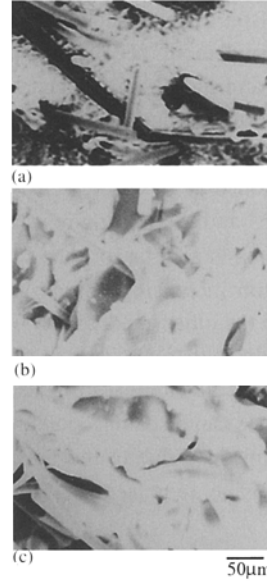


Fig. 8. Fracture surface of samples (a) A<sub>05</sub>, (b) B<sub>05</sub>, (c) C<sub>05</sub> at 25°C.

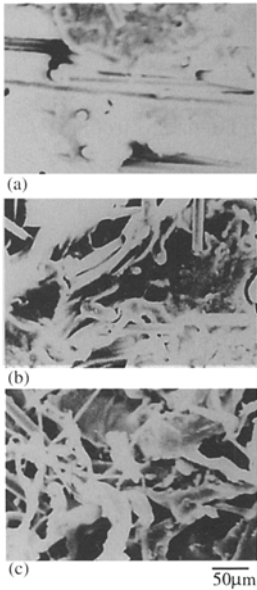


Fig. 9. Fracture surface of samples (a) A<sub>05</sub>, (b) B<sub>05</sub>, (c) C<sub>05</sub> at 0°C.

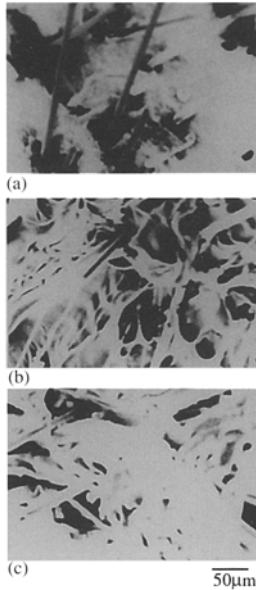


Fig. 10. Fracture surface of samples (a) A<sub>05</sub>, (b) B<sub>05</sub>, (c) C<sub>05</sub> at -20°C.

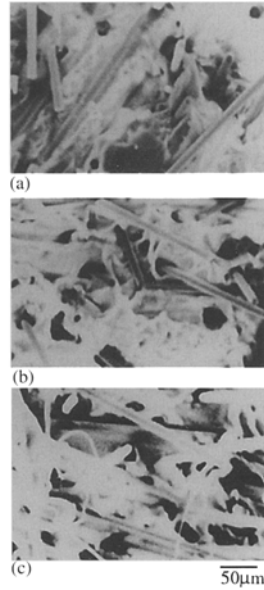


Fig. 11. Fracture surface of samples (a) A<sub>05</sub>, (b) B<sub>05</sub>, (c) C<sub>05</sub> at -50°C.

resins adhere better to titanate coupling agent than linear HDPE resins and the adhesion is better for SBPE resins associated with longer branch length. One possible explanation is that the entanglement between the thermoplastic functional group of titanate CA ( $(-\text{Ti}(-\text{OC}_8\text{H}_{17})_2)_3$ ) and short-chain branched molecules in amorphous regions may be firmer with increasing branch length, and the entanglement between  $\text{Ti}(-\text{OC}_8\text{H}_{17})_2$  and short-chain branched molecules in amorphous regions may be more and firmer than that of linear molecules, since tie molecule density associated SBPE resins is larger than that of linear HDPE resins and the pulling resistance of short-chain branched molecules through the entanglements is also larger than that of the linear molecules. It is, therefore, a higher adhesion with increasing branch length between PE resins and the carbon fibers was found. On the other hand, as shown in Figs. 9-11, more voids due to fiber pull-out, and less PE residue adhered to carbon fibers were found with decreasing temperature. This is possibly due to the fact that PE resins shrink more than carbon fibers do, and the adhesion at the interface can be damaged at low temperatures before any impact test performed, and hence,  $E_t$  improved due to the presence of 5% carbon fiber reduced significantly with decreasing temperature (see fig. 4).

### **References**

1. Domininghaus H (1984), *Gummi Faser, Kunststoffe*, 37 : 326, 37 : 386.
2. Carvalho WS, Bretas RES (1990) *Eur. Polym. J.*, 26 : 817.
3. Bosshard AW, Schlumpf HP (1985) "Plastics Additives Handbook", Gächter R, Müller H, Hanser, Munich Vienna New York, p. 405.
4. Lu XC, Wang XQ, Brown N (1988), *J. Mater. Sci.*, 23 : 643.
5. Yeh JT, Chen CY, Hong HS, *J. Mater. Sci.*, accepted for publication.
6. Yeh JT, Chen JH, Hong HS, *J. Appl. Polym. Sci.*, accepted for publication.
7. Bubeck RA, Baker HM (1982), *Polym.*, 23 : 1680.
8. Monte SJ, Sugerman G (1985), "Ken-React Reference Manual-Titanate, Zirconate and Aluminate Coupling Agents", Kenrich Petrochemicals, Inc., U. S. A., p. 20.
9. Pooter MD, Smith PB, Dohrer KK (1991), *J. Appl. Polym. Sci.*, 42 : 399.
10. Brown N, Ward IM (1986), *J. Mater. Sci.*, 18 : 1405.
11. Liu TM, Baker WE (1992), *Polym. Eng. Sci.*, 32 : 753.

Received: 27 May 1994/Revised version: 21 July 1994/

Accepted: 25 July 1994